



Effect of annealing temperature on some physical properties of MgB₂ by using the Hall probe ac-susceptibility method

A. Varilci^a, D. Yegen^b, M. Tassi^c, D. Stamopoulos^c, C. Terzioglu^{a,*}

^a Department of Physics, Faculty of Arts and Sciences, Abant Izzet Baysal University, 14280 Bolu, Turkey

^b Department of Medical Physics, Dr. A.Y. Ankara Oncology Education and Research Hospital, Ministry of Healthy of Turkey, 06460 Ankara, Turkey

^c Institute of Materials Science, National Center for Scientific Research, Demokritos, 15310 Ag. Paraskevi, Athens, Greece

ARTICLE INFO

Article history:

Received 15 May 2008

Received in revised form

2 April 2009

Accepted 16 July 2009

PACS:

61.10.-I

74.25.Ha

74.25.Sv

Keywords:

Metallic superconductors

Annealing temperature

Peak temperature

Inter-granular critical current density

Critical-state model

ABSTRACT

A commercially available powder of MgB₂ is used as starting material for the examination of the influence of the annealing temperature on the properties of this intermediate- T_c superconductor. We performed scanning electron microscopy (SEM) and Hall ac-susceptibility measurements as a function of temperature and ac-field amplitude on samples annealed at 650, 750, 850 and 950 °C. The imaginary part of ac-susceptibility measurements is used to calculate both the inter-granular critical current density, $J_c(T_p)$ and density of pinning force, $\alpha_j(0)$. It was observed that all T_c , $J_c(T_p)$ and $\alpha_j(0)$ exhibit a non-monotonic behavior on the annealing temperature range studied in this work. T_c is measured to be 39.85 ± 0.02 K and $J_c(T_p)$ is estimated to be as high as 60 A/cm^2 at 39.2 K for the sample annealed at 850 °C. The peak temperature, T_p , in the imaginary part of the ac-susceptibility curves shifts to lower temperatures with both decreasing the annealing temperature and increasing the amplitude of the ac-magnetic fields. A comparison of the experimental ac-susceptibility data with theoretical critical-state models that are currently available is performed. SEM investigations showed that the grain size increases, and the grain connectivity improves when the annealing temperature increases up to 850 °C. The possible reasons for the observed changes in transport, microstructure and magnetic properties due to annealing temperature are discussed.

© 2009 Elsevier B.V. All rights reserved.

1. Introduction

Extensive research efforts have been dedicated towards the synthesis and study of MgB₂ metallic superconductors ever since its discovery by Nagamatsu et al. in 2001 [1]. One of the main reasons of excitement on this newly discovered intermediate- T_c MgB₂ superconductor is that the grain boundaries do not act as weak links which cause current limitations [2]. A vast amount of experimental investigations were executed to improve the properties of MgB₂ by modifying the preparation conditions [3–11] and study the properties of the vortex matter phase diagram [12–14]. Modifications in the lattice parameters, critical transition temperature, critical current density and microstructure characteristics were observed upon variation of the preparation conditions. Several investigations [15–17] have made clear that the MgB₂ superconductor may have critical current density (J_c) as high as 10^6 A/cm^2 . The magnetic induction [18] rather than the transport method [19] is the one that is most commonly used for the estimation of the critical current

density, J_c . Referring to magnetization measurements, the most favorite technique is the conventional ac-susceptibility method by means of mutual inductance coils [20] since it can be easily built in any ordinary research laboratory. However, a rough disadvantage of the mutual inductance coils method is that it exclusively provides bulk information on the whole specimen under investigation, thus not allowing to distinguish different irreversibility mechanisms such as bulk pinning of vortices and surface barriers [21,22].

On the contrary, the more delicate Hall probe ac-susceptibility method (diamagnetic shielding) can give information on a local region of a superconducting specimen owing to the small active area of the employed Hall sensor. Depending on the patterning technique the active area ranges from the micrometer to the millimeter scale, typically within 10×10 to $1000 \times 1000 \mu\text{m}^2$. Thus, this technique has been successfully employed for the study of very small single crystals of high- T_c superconductors, such as HgBa₂CuO_{4+ δ} and YBa₂Cu₃O_{7- δ} ultimately allowing to identify different irreversibility mechanisms that are simultaneously active during every experiment [23–28]. Also, the study of pinning properties as well as the vortex dynamics by miniature Hall probe ac-susceptibility can give local information about the intra-grain and inter-grain J_c .

* Corresponding author. Tel.: +90 3747 2541000; fax: +90 374 2534642.
E-mail address: terzioglu_c@ibu.edu.tr (C. Terzioglu).

In this work, we report on the results of Hall probe ac-susceptibility measurements under different ac-magnetic field amplitudes and scanning electron microscopy (SEM) data. From the ac-susceptibility measurements, we estimated the temperature dependence of the inter-granular critical current density as a function of the annealing temperature using Bean's model and studied the peak temperature dependence as a function of ac-magnetic field amplitude, in order to investigate the effect of annealing temperature on the inter-granular pinning force. Detailed simulations have been performed by employing well-established theoretical propositions that are based on the critical-state model [29,30]. In addition we investigated the microstructure characteristics of the samples that were annealed at various temperatures by performing detailed SEM measurements.

2. Experimental detail

A commercially available powder of MgB_2 (Alfa Aesar) was used as starting material for the preparation of MgB_2 superconducting samples that were annealed at 650, 750, 850 and 950 °C. The heat treatments were carried out in flowing Ar gas for 2 h. The samples were wrapped with Ta foil to reduce the interaction between sample and quartz tube in the furnace during heat treatments and to minimize the influence of any residual O_2 since it is well known that Ta is a very efficient O_2 getter. The MgB_2 samples investigated in our Hall ac-susceptibility experiments were disk shaped with thickness of 2 mm and diameter of 5 mm. An axial Hall sensor from Lakeshore Company was used in this work which has a magnetic sensitivity of 0.55 mV/kG and diameter of the active area 0.8 mm. The typical value of the current applied to the Hall sensor was 200 mA. The temperature of the samples was recorded by means of a Si diode. The uncertainty of temperature measurements is about 20 mK. A cryostat from Oxford Company was used for our measurements. Typically, our measurements were performed in a dynamic mode, starting at 30 K with heating rate of 1 K/min and data were recorded in the temperature range between 35 and 45 K. The amplitudes of the ac-magnetic field investigated during these experiments were 240, 480, 720, 960 and 1200 A/m. The frequency was kept constant at 20 Hz. Susceptibility data taken by means of a lock-in amplifier were recorded by using the Labview software. Since the signal generated by the Hall sensor is very weak a Tegam (model 73) precision ratio transformation is used for farther amplification. Fig. 1 shows a schematic illustration of the Hall probe ac-susceptibility set-up. The complex ac-magnetic induction detected by the Hall sensor depends on the penetration of the applied ac-magnetic field in the superconductor, thus ultimately giving information on the shielding ability of the specimen under investigation. Details on the experimental set-up and sample preparation can also be found elsewhere [31].

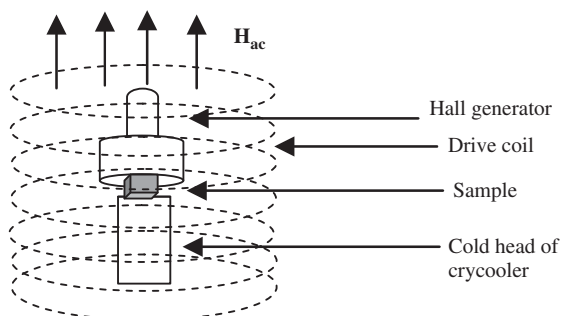


Fig. 1. Hall probe ac-susceptibility measurement system.

The surface morphology and microstructure of the samples were investigated by the JEOL 6390-LV SEM.

3. Results and discussions

In our previous study [32], we investigated the effect of annealing temperature on the crystalline structure, magnetic and mechanical properties of MgB_2 superconducting samples by employing XRD data, ac-susceptibility experiments and Vickers microhardness measurements. These investigations showed that the increase in annealing temperature from 650 to 850 °C increased lattice parameters, critical transition temperature, microhardness values and improved the grain connectivity. It was also observed that the Vickers microhardness of the samples depends on the applied load. In addition, we calculated the load dependent mechanical properties of the samples such as Young's modulus, yield strength and fracture toughness. They were also found to be annealing temperature and load dependent.

In the present study, we have performed ac-susceptibility measurements as a function of temperature and ac-magnetic field amplitude by using the local Hall probe method. The samples of MgB_2 disks discussed in this work will be hereafter denoted as M650, M750, M850 and M950 since they were annealed at 650, 750, 850 and 950 °C, respectively, for 1 h under Ar gas flow. The real and imaginary components of the ac-susceptibility curves are shown as a function of temperature and ac-magnetic field amplitude in Fig. 2 for the MgB_2 superconductor samples annealed at different temperatures. The signal detected by the Hall sensor is related to the shielding ability of the sample. The transition temperatures at a 240 A/m ac-magnetic field for samples M650, M750, M850 and M950, are 38.66, 39.46, 39.85 and 39.66 K, respectively. It is observed that the critical temperature exhibits a non-monotonic dependence on the annealing temperature since it is maximized for the M850 sample. From the above results, it was inferred that the annealing temperature can be used to optimize the critical temperature T_c value of the MgB_2 samples. It was also observed that the characteristics of the ac-susceptibility curves depend on the annealing temperature. The superconducting transition width of the M650, M750 and M950 samples ($\Delta T = 3$ K) is about three times larger than that of M850 sample ($\Delta T = 1$ K). The bulk nature of superconductivity is confirmed by observation of well-defined single-step transition and large shielding fracture for the M850 sample. The reduction in the width of the ac-susceptibility curve observed in the M850 sample may be due to microstructure changes and increase in the contact area among the superconducting grains induced by the optimum annealing temperatures. This behavior probably reflects the improvement of the coupling between superconducting grains.

In the imaginary part of the ac-susceptibility curves, there are usually two peaks that relate to the intrinsic (intra-grain behavior observed for low amplitudes of the ac-magnetic field) and extrinsic (inter-grain behavior observed for relatively high amplitudes of the ac-magnetic field) properties of the superconducting grains that form the specimen under investigation. No intra-grain peak arising from the irreversible motion of vortices inside the grains was observed in the present work. The loss peak observed in the imaginary part of the ac-susceptibility curves relates to the coupling between neighboring grains (inter-grain behavior) and is suppressed for the M650 sample, while is quite pronounced for all other samples. This particular peak indicates the maximum hysteresis loss due to inter-grain motion of vortices. As can be seen in Figs. 1(a)–(d), the real part of the ac-susceptibility curves shifts to lower temperatures and its width increases with (i) increasing ac-magnetic field amplitudes from

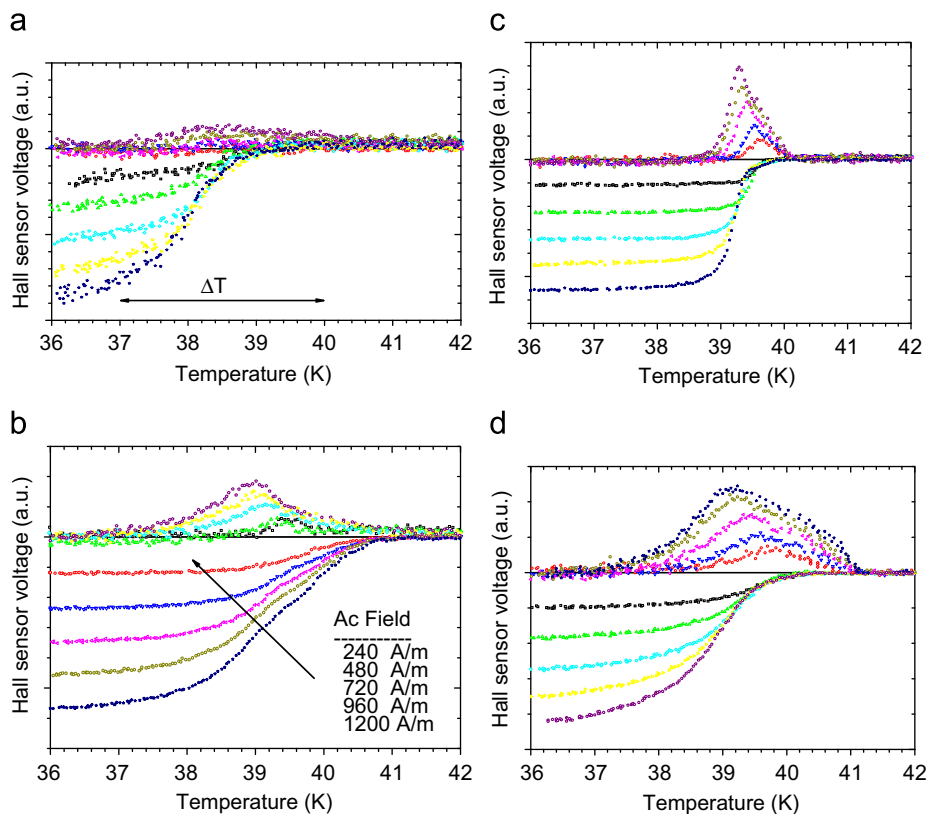


Fig. 2. Real and imaginary parts of ac-susceptibility of MgB₂ samples annealed at (a) 650, (b) 750, (c) 850 and (d) 950 °C.

240 to 1200 A/m and (ii) decreasing annealing temperature from 850 to 650 °C. On the other hand the inter-granular peak of the imaginary part of the ac-susceptibility curves shifts to lower temperatures and broadens as the ac-magnetic field increases from 240 to 1200 A/m. The amount of the shift as a function of ac-field amplitude is proportional to the strength of the pinning force [33]. In addition, the intensity of the imaginary part increases with increasing ac-field amplitude. This is associated with the irreversible flux penetration into the inter-grains of superconducting MgB₂. Moreover, the imaginary part of the ac-susceptibility curves for the M650, M750 and M950 samples shows a slightly broader coupling with a substantial shift to lower temperatures and with smaller amplitude. This means that these particular samples have a weaker pinning force. On the contrary, in the M850 sample the coupling between neighboring grains is strong so that narrower coupling peaks are obtained, ultimately indicating a higher pinning force. This finding is supported by the peak temperature dependence as a function of ac-magnetic field investigations and the respective critical current density calculations as explained below. Hence, the conclusion based on the results of ac-susceptibility investigations presented here might be that the M850 sample is a better candidate than the M650, M750 and M950 samples, especially in high-field and current-carrying applications.

In order to study the influence of annealing temperature on the inter-granular pinning force, the loss peak temperature dependence of the imaginary curves as a function of ac-magnetic field, H_{ac} , has been investigated. Fig. 3 presents the ac-magnetic field dependence of loss peaks, T_p , for samples annealed at the four characteristic temperatures. By adopting the critical state model, Muller [34] found that T_p is linearly proportional to H_{ac} but inversely proportional to the inter-granular pinning force density. Muller's critical state model assumes a magnetic-

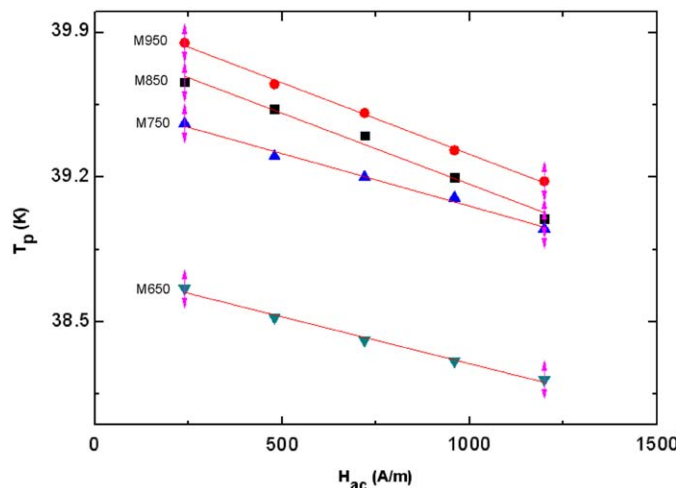


Fig. 3. Inter-granular peak temperature vs ac-magnetic field amplitude for the M650, M750, M850 and M950 MgB₂ samples.

flux-independent pinning force density where the α_j and α_g for inter- and intra-granular vortices are described by the relation [34]

$$T_p = T_{p0} - T_{p0} U^{1/2} H_{ac} \quad (1)$$

where U is $[\mu_0 \mu_{eff}(0) / 2a\alpha_j(0)]$, a is the length of the samples, $\mu_{eff}(0)$ is the effective permeability of the ceramic and $\alpha_j(0)$ is the inter-granular pinning force density. As clearly seen from the figure, each set of data shows an excellent linear relationship between T_p and H_{ac} for all samples. The slope of each line is proportional to

Table 1
The extracted values of T_{p0} , and U of the MgB₂ samples.

Samples	T_{p0} (K)	$U ((\alpha_f(0))^{-1/2})$
M950	39.85	6.88×10^{-4}
M850	40.00	6.92×10^{-4}
M750	39.57	5.08×10^{-4}
M650	38.75	4.54×10^{-4}

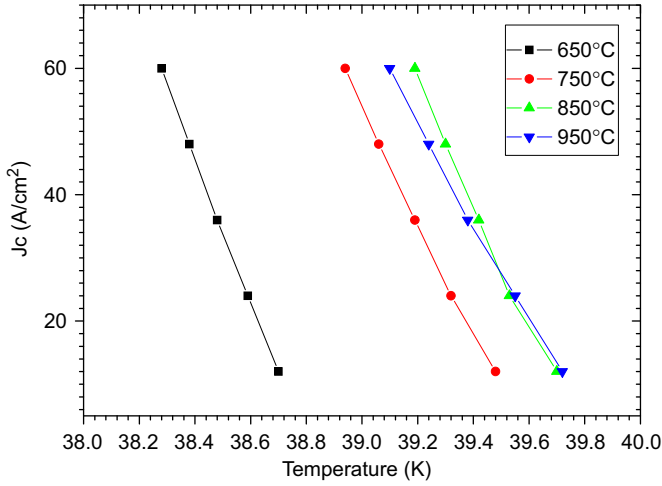


Fig. 4. Granular critical current density vs temperature for the M650, M750, M850 and M950 MgB₂ samples.

$(\alpha_f(0))^{-1/2}$ and the vertical intercept of each line corresponds to the peak temperature, T_{p0} , at zero ac-magnetic field amplitude. From a least squares fitting procedure by using Eq. (1) the data T_{p0} and U were estimated for all samples and tabulated in Table 1. As can be seen from the table, the values of T_{p0} increased, while U decreased with increasing annealing temperature. A decreasing trend in U means that the values of $\alpha_f(0)$ increase with increasing of the annealing temperature. A decreasing trend in pinning force of the samples with decreasing annealing temperature can be attributed to greater voids and defects. This finding is supported by inter-granular critical current density and SEM results.

As mentioned before, the peak position of the imaginary curves shifts to low temperatures for higher ac-magnetic field amplitudes. From the positions of the peaks, the inter-granular critical current densities J_c^{inter} at the peak temperatures (T_p) can be calculated using Bean's "loss peak maximum" method [29]. In Fig. 4, magnetically estimated critical current densities for only inter-grain region at temperatures close to T_c were plotted since there is no intra-grain peaks. The data of Fig. 4 were obtained as follows: When the imaginary part obtains its maximum value, full flux penetration occurs. At the peak temperature, T_p the magnetically estimated J_c^{inter} is given by $J_c^{inter}(T_p) = H_{ac}/a$, where H_{ac} is the ac-magnetic field amplitude and a is the thickness of the sample. As seen from the figure, the critical current density is greatly affected by the annealing temperature. The sample annealed at 850 °C has higher J_c^{inter} (60 A/cm² at 39.2 K) than the other samples.

This can be farther elaborated by comparing our experimental data with well-established theoretical propositions that refer to the ac-susceptibility of type-II superconductors as was studied by Shatz et al. in Ref. [30]. In that work the authors derived the general expressions for the harmonic ac-susceptibilities (see Ref. [30, Table 1]) by taking into account various models referring to the dependence of the critical current density on the externally

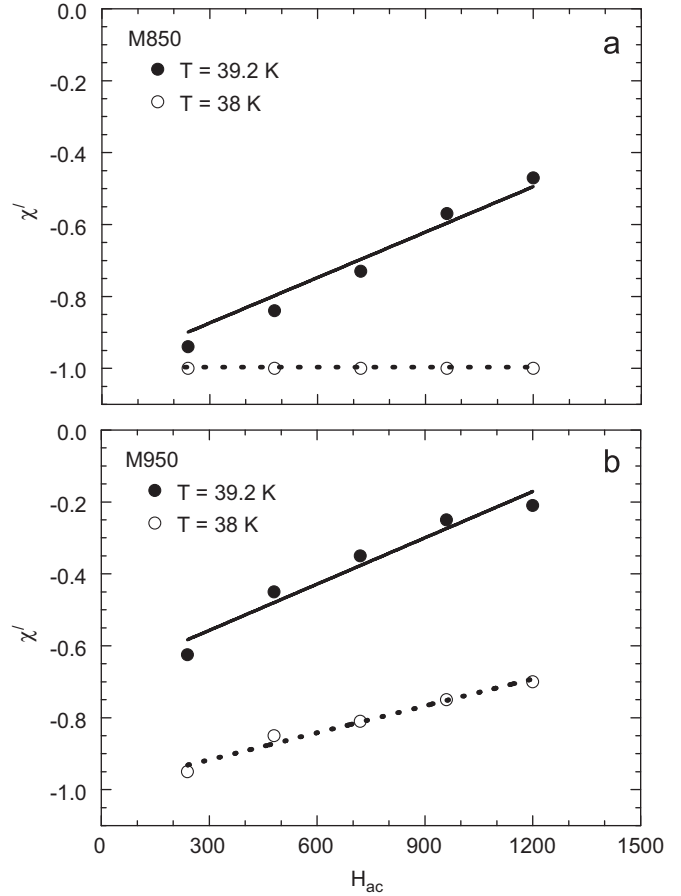


Fig. 5. Comparison of the first harmonic ac-susceptibility experimental data with the theoretical expressions obtained in Ref. [30].

applied dc-magnetic field, namely the Bean, the Kim-Anderson and the power-law ones. Strictly speaking our limited experimental results can be compared with the more general theoretical propositions of Ref. [30] only for the specific case where the externally applied dc-magnetic field is zero since our current data refer to this specific case. However, by making reasonable assumptions the comparison results in rational conclusions as is illustrated in Fig. 5 where we examine representative ac-susceptibility data that refer to the samples M850 (panel (a)) and M950 (panel (b)). The two other samples, namely M650 and M750, showed the same behavior as sample M950. The experimental data points refer to the variation of the first harmonic ac-susceptibility upon the amplitude of the ac-magnetic field for constant temperature, while the fitting lines refer to the theoretical first harmonic linear Bean model expression, $\chi' = -1 + H_{ac}/H^*$ where $H^* = 4\pi\alpha J_c/c$ originally supplied in Table 1 and Appendix A.1 of Ref. [30]. We note that these experimental data were obtained from that presented in Figs. 2(a)–(d) by assuming that complete shielding is achieved at the lowest temperature where the measurements initiate, i.e. at $T = 36$ K. We also stress that in our estimations α refers to the radius of the Hall sensor active area, i.e. 0.4 mm, since these local ac-susceptibility experiments exclusively detect the signal at the active area of the Hall sensor and not that of the whole disk-shaped sample. In Figs. 5(a) and (b) two characteristic temperatures of the experimental data set are presented, $T = 38$ and 39.2 K. We observe that the fitting of the experimental data is quite suitable. We note that for the sample M850 the linear fitting curves were forced to cross the -1 susceptibility value, as should

be, for both temperatures, while for the M950 one this holds for only the data set referring to $T = 38$ K. For $T = 39.2$ K the estimation of the H^* parameter was performed on the more simple basis of a least-square fitting optimization. The critical current density values as estimated from these data range within 20 and 50 A/cm². Thus, the results obtained by comparing with the theoretical propositions of Ref. [30] are in fair agreement with the ones obtained right above by means of the alternative theoretical propositions of Ref. [29].

Referring to practical applications we should now unveil the mechanism responsible for the higher critical current density observed in the M850 sample. Probably the relatively high annealing temperature (850 °C), in comparison to the M650 and M750 samples, results in a single phase for the M850 one, which exhibits good grain connectivity ultimately enabling high J_c^{inter} values [35]. On the other hand what is the mechanism that reduces the critical current density for the sample M950, 75 A/cm² at 39.34 K, which is annealed at an even higher temperature? We know from our previous XRD investigations that the M950 sample has an impurity phase of B. Existing impurities would apparently deteriorate its $J_c^{inter}(T_p)$ value. Resultantly, annealing temperature is a parameter to be controlled for increasing the grain connectivity and inter-granular critical current density.

The surface morphology of the MgB₂ samples was studied by SEM in order to determine and compare the grain sizes. The surface micrographs for the samples annealed at different annealing temperatures are displayed in Fig. 6. When the sample is annealed at 850 °C, its microstructure is remarkably different from that of annealed at 650 and 750 °C. As seen from the figure, the reaction between Mg and B is incomplete in the M650 and M750 samples. Meanwhile, numerous small grains become visible in the grain boundaries. It reveals that the grains are not well connected in the surface for the samples annealed at 650 and 750 °C. However, the grains of the sample annealed at 850 °C are well connected. Furthermore, a broad grain size distribution can be seen for the sample annealed at 850 °C, which is in good agreement with the XRD results presented in a previous study of ours [32]. The grain sizes are about 100–120 nm

for the sample M850. This value is consistent with grain size calculated using Scherrer–Warren equation from the full-width at half maximum of the XRD peaks. It is observed that the grain connectivity is greatly enhanced with increasing the annealing temperature from 650 to 850 °C. The surface of the M850 sample is also denser. The increase of T_c in the samples may also be caused by the increase of grain sizes and their orientations, by improved coupling between superconducting grains, and by the increased number of flux pinning centres. M650 and M750 have a non-uniform surface appearance with smaller grains. From these SEM data one can say that the grains in the M650, M750 samples are randomly oriented and poorly connected. Finally, the grain size of the sample M950 is similar to that of M850 but shows more signs of partial melting due to the higher annealing temperature. We could assume that sublimation of Mg occurred at the grain boundaries where the internal energy of the crystal is higher. As a result, accumulation of segregated B also occurred at the grain boundaries. This finding can be related to the ac-susceptibility measurements as discussed above.

4. Conclusions

We have investigated the magnetic behavior of MgB₂ samples annealed at 650, 750 850 and 950 °C by means of the Hall ac-susceptibility method as a function of temperature and ac-magnetic field. The maximum temperature T_p in the imaginary ac-susceptibility curves shifts slightly to lower temperatures with increasing ac-magnetic field from 240 to 1200 A/m as well as with decreasing of the annealing temperature. The critical temperature is found to increase from 38.66 to 39.85 K at 240 A/m by increasing the annealing temperature up to 850 °C, along with sharpening of the respective ac-susceptibility curve. The annealing temperature improves the coupling characteristics between superconducting grains, the grain connectivity and these lead to a higher critical temperature. The highest value of inter-grain critical current density is registered after annealing at 850 °C. This result is attributed to microcrack eliminations and good grain

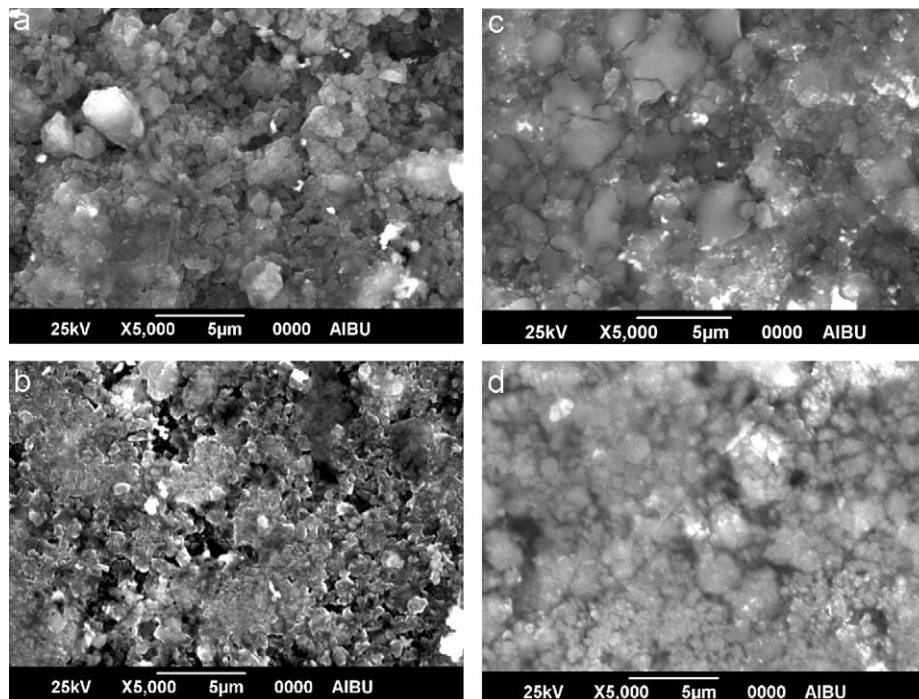


Fig. 6. SEM micrographs of the (a) M650, (b) M750, (c) M850 and (d) M950 MgB₂ samples.

connectivity. The shielding due to the inter-grain current occurs at much lower temperature for the M650, M750 and M950 samples as compared to M850 sample, indicating the high quality grain connectivity in M850 sample. The transport, magnetic and microstructure properties are remarkably enhanced with increasing annealing temperature obtaining their optimum values at 850 °C. Hence the conclusion based on the comparative results of ac-susceptibility and SEM investigations presented here is that the M850 sample is a better candidate than the M650, M750 and M950 samples as far as high-field and current-carrying applications are considered.

Acknowledgments

This work is financially supported by the Scientific and Technological Council of Turkey (Project no: 104T324) and partly by the Turkish State Planning Organization (Project no: 2004K120200).

References

- [1] J. Nagamatsu, N. Nakagawa, T. Muranaka, Y. Zenitani, J. Akimitsu, *Nature* 410 (2001) 63.
- [2] T.S. Kayed, *Cryst. Res. Tech.* 39 (2004) 50.
- [3] N.N. Kolesnikov, M.P. Kulakov, *Physica C* 363 (2001) 166.
- [4] H. Takano, H. Kokubo, T. Kinami, Y. Amakai, S. Murayama, *J. Magnetism Magnetic Mater.* 310 (2007) e134.
- [5] T. Wu, J.K.F. Yau, Y.M. Cai, Y.G. Cui, D.W. Gu, P.F. Yuan, G.Q. Yuan, L.J. Shen, X. Jin, *Physica C* 386 (2003) 638.
- [6] A. Yamamoto, J. Shimoyama, S. Ueda, Y. Katsura, I. Iwayama, S. Horii, K. Kishio, *Physica C* 426–431 (2005) 1220.
- [7] F. Qing-rong, C. Chinping, X. Jun, K. Ling-wen, C. Xin, W. Yong-zhong, Z. Yan, G. Zheng-xiang, *Physica C* 411 (2004) 41.
- [8] A. Matsmoto, H. Kumakara, H. Kitaguchi, H. Fuji, K. Tugano, *Physica C* 382 (2002) 207.
- [9] D.K. Aswal, S. Sen, A. Singh, T.V. Chandrasekhar Rao, J.C. Vyas, L.C. Gupta, V.C. Sahni, *Physica C* 363 (2001) 149.
- [10] G.J. Xu, R. Pinholt, J. Bilde-Sorensen, J.-C. Grivel, A.B. Abrahamsen, N.H. Andersen, *Physica C* 434 (2006) 67.
- [11] H. Abe, M. Naito, K. Nogi, M. Matsuda, M. Miyake, S. Ohara, A. Kondo, T. Fukui, *Physica C* 391 (2003) 211.
- [12] M. Pissas, D. Stamopoulos, S. Lee, S. Tajima, *Phys. Rev. B* 70 (2004) 134503.
- [13] M. Pissas, D. Stamopoulos, N. Zhigadlo, J. Karpinski, *Phys. Rev. B* 75 (2007) 184533.
- [14] M. Pissas, D. Stamopoulos, S. Koutantos, *J. Supercond.* 17 (2004) 259.
- [15] C.B. Eom, M.K. Lee, J.H. Choi, L.J. Belenky, X. Song, L.D. Cooley, M.T. Naus, S. Patnaik, J. Jiang, M. Rikel, A. Polyanskii, A. Gurevich, X.Y. Cai, S.D. Bu, S.E. Babcock, E.E. Hellstrom, D.C. Larbalestier, N. Rogado, K.A. Regan, M.A. Hayward, T. He, J.S. Slusky, K. Inumaru, M.K. Haas, R.J. Cava, *Nature* 411 (2001) 558.
- [16] D.N. Zheng, J.Y. Xiang, P.L. Lang, J.Q. Li, G.C. Che, Z.W. Zhao, H.H. Wen, H.Y. Tian, Y.M. Ni, Z.X. Zhao, *Physica C* 408–410 (2004) 136.
- [17] K.M. Elsabawy, E.E. Kandyel, *J. Mater. Res. Bull.* 42 (2007) 1051.
- [18] M. Kiuchi, H. Mihara, K. Kimura, T. Haraguchi, E.S. Otobe, T. Matsushita, A. Yamamoto, J. Shimoyama, K. Kishio, *Physica C* 445–448 (2006) 474.
- [19] H. Kumakura, A. Matsumoto, T. Nakane, H. Kitaguchi, *Physica C* 456 (2007) 196.
- [20] S.K. Agarwal, B.V. Kumaraswamy, *J. Phys. Chem. Solids* 66 (2005) 729.
- [21] A.M. Campbell, *J. Phys. C—Solid State Phys.* 2 (1969) 1492.
- [22] R.W. Rollins, H. Kupfer, W. Gey, *J. Appl. Phys.* 45 (1974) 5392.
- [23] D. Stamopoulos, M. Pissas, *Physica C* 332 (2000) 456.
- [24] D. Stamopoulos, M. Pissas, *Physica B* 284–288 (2000) 805.
- [25] D. Stamopoulos, M. Pissas, *Supercond. Sci. Tech.* 14 (2001) 844.
- [26] D. Stamopoulos, M. Pissas, *Phys. Rev. B* 65 (2002) 134524.
- [27] D. Stamopoulos, M. Pissas, *Phys. Rev. B* 64 (2001) 134510.
- [28] D. Stamopoulos, M. Pissas, *Phys. Rev. B* 66 (2002) 214521.
- [29] C.P. Bean, *Phys. Rev. Lett.* 8 (1962) 250.
- [30] S. Shatz, A. Shaulov, Y. Yeshurun, *Phys. Rev. B* 48 (1993) 13871.
- [31] A. Varilci, *Supercond. Sci. Tech.* 20 (2007) 397.
- [32] C. Terzioglu, A. Varilci, I. Belenli, *J. Alloys Comp.* 478 (2009) 836.
- [33] H. Salamati, P. Kameli, *Solid State Commun.* 125 (2003) 407.
- [34] K.H. Muller, S.J. Collocott, R. Driver, *Physica C* 191 (1992) 339.
- [35] V.A. Drozd, A.M. Gabovich, P. Gierowski, M. Pezkała, H. Szymczak, *Physica C* 402 (2004) 325.